Evaluation of Cerebral Infarction with Iodine-123-Iomazenil SPECT

Jun Hatazawa, Takao Satoh, Eku Shimosegawa, Toshio Okudera, Atsushi Inugami, Toshihide Ogawa, Hideaki Fujita, Kyo Noguchi, Iwao Kanno, Shuhichi Miura, Matsutaroh Murakami, Hidehiro Iida, Yuhko Miura and Kazuo Uemura

Department of Radiology and Nuclear Medicine, Akita Research Institute of Brain and Blood Vessels, Senshuh-Kubota Machi, Akita, Japan

This study evaluates ischemic damage to central benzodiazepine (BZD) receptor binding in the brain with [^{123}I]iomazenil SPECT in relation to CT hypodense lesions and blood flow abnormalities. **Methods:** Nine patients with middle cerebral artery territory infarction were studied. Iomazenil images obtained 180 min postinjection were analyzed for BZD receptor binding. The cortical infarction, visualized as CT hypodense area on CT, the peri-infarct area, visualized as normodensity surrounding the infarction on CT, the intrahemispheric remote area and the cerebellum were analyzed by taking the ratio of the lesion to contralateral mirror region (L/C ratio). CT during the chronic stage and perfusion images obtained during the smallest time difference between the two studies were used for comparative analysis. **Results:** The mean L/C ratio of iomazenil uptake was 0.53 ± 0.08, 0.79 ± 0.07, 0.98 ± 0.03 and 1.00 ± 0.04 in the infarct, peri-infarct and remote areas and the cerebellum, respectively. The infarct and peri-infarct areas showed significant decrease compared with unity. The corresponding mean L/C ratio for blood flow was 0.52 ± 0.08, 0.73 ± 0.07, 0.83 ± 0.09, and 0.80 ± 0.07, respectively. In all areas, the ratios were significantly decreased compared with unity. There was significant difference between the L/C ratio for blood flow and iomazenil in the remote area and the cerebellum. **Conclusion:** Iodine-123-iomazenil SPECT imaging may provide new information on ischemic damage to the brain, particularly to neurons.

Key Words: single-photon emission computed tomography; benzodiazepine receptors; iodine-123-iomazenil; cerebral infarction

J Nucl Med 1995; 36:2154–2161

A number of imaging techniques have been used to visualize ischemic damage to the brain. Of these, CT and MRI are sensitive to edematous change in the early stage of brain ischemia and localize ischemic necrosis at the chronic stage (*1,2*). Perfusion imaging revealed the severity and extent of disturbed blood flow at a very early stage (*3*) and predicted the clinical outcome (*4*). By measuring perfusion and metabolism, the balance of the supply and demand of substrates (i.e., misery or luxury perfusion) was evaluated (*5*). Nevertheless, these imaging modalities are unable to provide direct information on neuron-specific damage after ischemic insult.

Recently, Sette et al. performed in vivo mapping in the baboon of the central benzodiazepine (BZD) receptor after focal ischemia with PET and ^{11}C-flumazenil (*6*). The central BZD receptor exists with variable density in the membrane of neurons. Carbon-11-flumazenil is a ligand which binds specifically to the central BZD receptor. The study demonstrated decreased binding of ^{11}C-flumazenil to the central BZD receptor in the infarct and peri-infarct lesions. It was suggested that the decrease in central BZD receptor binding may reflect damage to synapses and may therefore be sensitive to neuronal injury due to ischemia.

Iodine-123-Ro 16-0154 (ethyl-5,6-dihydro-7-iodo-5-methyl-6-oxo-4H-imidazo[1,5-a][1,4]-benzodiazepine-3-carboxylate; iomazenil) is a SPECT tracer developed for central BZD receptor imaging (*7–10*). The ligand is highly selective, with an affinity tenfold greater than that of ^{11}C-flumazenil. Dosimetry estimates for [^{123}I]iomazenil, based on human biodistribution data, were found to be within the dose range acceptable in clinical studies (*11*). With this ligand, it is now possible to study central BZD receptor binding in patients with cerebral infarction with SPECT. The purpose of this study was: (a) to visualize the changes in central BZD receptor binding in the infarct, peri-infarct and nonischemic remote areas, (b) to compare the abnormality in central BZD receptor binding with the CT lesion and blood flow abnormality and (c) to assess lesion localization with iomazenil SPECT imaging in aphasic patients.

MATERIALS AND METHODS

Patients

Nine patients (6 men, 3 women, aged 51–63 yr, mean 58.8 ± 3.7 yr) with cerebral infarction in the middle cerebral artery (MCA) territory were examined. Seven patients had cortical infarction resulting from a trunk or branch occlusion of the MCA. Two patients (nos. 7 and 8) had CT hypodensity only in the subcortical white matter, with normal appearance of the adjacent cortex. One patient (no. 5) had both cortical and subcortical white matter

Received Oct. 19, 1994; revision accepted Feb. 14, 1995.

For correspondence or reprints contact: Jun Hatazawa, MD, PhD, Department of Radiology and Nuclear Medicine, Akita Research Institute of Brain and Blood Vessels, 6-10 Senshu-Kubota Machi, Akita City, Akita, Japan 010.

TABLE 1
Clinical Data

Patient no.	Age	Sex	Infarction location	Cortical signs during iomazenil study	Time of study after onset		
					SPECT (days)	Blood flow (days)	PET (days)
1	63	F	Cortical, l. parietal	Global aphasia	4	1	44
2	61	M	Cortical, r. parietal	Apraxia	8	n.a.	n.a.
3	61	M	Cortical, r. temporal	Hemianopsia	9	16	n.a.
4	51	F	Cortical, r. temporal	None	10	4	n.a.
5	61	M	Cortical, l. frontal Subcortical, l. temporal	Motor aphasia	19	n.a.	n.a.
6	59	M	Cortical, l. temporal	Sensory aphasia	35	38	n.a.
7	61	M	Subcortical, l. frontal	Global aphasia	46	40	n.a.
8	54	F	Subcortical, r. frontal	None	49	n.a.	82
9	58	M	Cortical, r. temporal	None	196	n.a.	167

n.a. = not available.

infarction in different brain regions. These lesions were analyzed separately.

For Patient 1, the iomazenil SPECT study was performed during the acute stage 4 days after onset (= Day 0). In four patients, studies were performed during the subacute phase from 2 to 3 wk after onset. The other four patients were examined during the chronic phase, from 35 days to 196 days after onset. Clinical data are summarized in Table 1. None of the patients had experienced cerebrovascular disease before the present attack. Seven of nine patients (nos. 1, 2, 4, 5, 6, 8, and 9) suffered from hemiparesis of the contralateral side of their brain lesion during the SPECT study. Patient 3 showed sensory disturbance of the left side. No patient was treated with a BZD receptor agonist such as diazepam before the iomazenil study. Written informed consent was received from all patients prior to study initiation.

Radioligand

Patients received approximately 165 MBq [^{123}I]iomazenil by intravenous bolus injection of 1.5 ml of solution into a cubital vein. Specific activity was approximately 222 MBq/μg at administration, resulting in an injected dose of 0.75 μg. Prior to the study, patients orally received potassium chloride to avoid thyroid contamination from the administered radioactivity.

Morphological Evaluation of Infarction

All patients underwent repeat serial CT over the clinical course. Ten axial images with 10-mm slice thickness and 10-mm center-to-center spacing were obtained parallel to the orbitomeatal (OM) line. To compare iomazenil binding, the CT scan taken during the chronic stage was selected as a reference to designate the final topography of the infarction. CT images were transferred to a conventional UNIX workstation system (TITAN 750, Kubota Computer Corp., Tokyo, Japan) for comparison with the SPECT data.

SPECT

A ring-type single-photon emission computed tomograph (Headtome SET-080, Shimadzu Co., Kyoto) was used to measure radioactivity distribution in the brain. The scanner simultaneously produces 31 tomographic axial slices. A low-energy, all-purpose collimator was used for data acquisition. Data were recorded on a 64 × 64 matrix. A Butterworth filter, cutoff 0.45 Nyquist and order 3, and a ramp filter were used for image reconstruction. Reconstructed images were corrected for tissue absorption using an attenuation coefficient of 0.125 cm^{-1}. In-plane and axial spatial resolution of the scanner were 14 and 22 mm FWHM, respectively. To evaluate initial tracer uptake to the brain, a dynamic SPECT study, seven scans with 3 min of data acquisition followed by seven scans with 6 min of data acquisition, was initiated with iomazenil administration. Final SPECT imaging was started 180 min postinjection, with 12 min of data acquisition. The plane of the CT and iomazenil imaging was set parallel to the OM line. All image data were transferred to a conventional UNIX workstation.

Evaluation of Central BZD Receptor Binding of Iodine-123-Iomazenil

Iodine-123-iomazenil SPECT images obtained 180 min postinjection were used to analyze central BZD receptor distribution. The area of cortical infarction was identified as the CT hypodense lesion (n = 7). The peri-infarct area was defined as the CT normodense area surrounding the cortical infarction or the cortex adjacent to the subcortical white matter infarction within the MCA territory. In Patient 3, CT hypodensity extended over the whole MCA territory and a peri-infarct area could not be identified. A total of nine lesions served as the peri-infarct area.

The superior frontal gyrus, a territory of the anterior cerebral artery, was defined as the remote area of the infarction (n = 9). The cerebellum also served as a remote area. No patient had CT evidence of a local morphological abnormality in the superior frontal gyri and cerebellum bilaterally. Image counts of the infarcted and the peri-infarct areas, the superior frontal gyrus, as well as their mirror regions, were read using a 16-mm diameter circular region of interest (ROI). The CT and SPECT images were not fused in this analysis. Instead, the ROI's position was determined manually as follows: The CT image which most depicted the infarction was first displayed on the left half field of the monitor of a workstation. Then, the early SPECT images obtained 15 min postinjection were displayed on the right half of the monitor. Because the early images depicted the landmark structures of the cerebrum, such as the basal ganglia and thalamus, they were used to match the iomazenil image with the corresponding CT image. ROIs for the infarcted area, peri-infarct area, superior frontal gyrus, cerebellum and their mirror regions were defined on the early iomazenil image by visual comparison with the CT image. The ROIs were finally superimposed on the SPECT images obtained 180 min after administration. The count ratio of the lesion-to-contralateral mirror region was defined as the L/C ratio. For the

cerebellum, an irregular ROI encompassing the cerebellar hemisphere was drawn manually. The contralateral-to-ipsilateral count ratio was calculated to give the L/C ratio. Statistical significance was determined by a paired t-test and the one-sample Wilcoxon test. The L/C ratio was analyzed in relation to the age of the infarction for the seven cortical and nine peri-infarct areas to determine time-dependent changes in ischemic lesions.

Evaluation of Blood Flow

Blood flow imaging was performed using [^{123}I]IMP (Patients 1, 4, 6, 7), ^{99m}Tc-HMPAO (Patient 3) or ^{15}O-water (Patients 8, 9). From 111 to 167 MBq [^{123}I]IMP or 740 MBq ^{99m}Tc-HMPAO were administered per injection. SPECT perfusion images were obtained with the same scanner used in the iomazenil study along with a low-energy, all-purpose collimator for the [^{123}I]IMP study and a low-energy, high-resolution collimator for the ^{99m}Tc-HMPAO study. The ^{15}O-water PET study is described as follows: The imaging plane was adjusted until parallel to the OM line. All IMP studies were performed according to the autoradiographic method (*12*) to quantify cerebral blood flow. For the ^{99m}Tc-HMPAO images, linearization correction (*13*) was applied. Two patients (nos. 1 and 4) were studied during the acute stage. One patient (no. 3) was studied during the subacute stage. In the other four patients, iomazenil uptake and blood flow were measured during the chronic stage (35 to 196 days after onset). The L/C ratios of the blood flow images were calculated for the infarction, peri-infarct and intrahemispheric remote areas and the cerebellum corresponding to the iomazenil image.

PET Imaging of Cerebral Blood Flow and Oxygen Metabolism

Regional cerebral blood flow (rCBF), regional extraction fraction for oxygen (rOEF), regional metabolic rate for oxygen ($rCMRO_2$) and regional cerebral blood volume (rCBV) were measured in Patients 1, 8 and 9 during the chronic stage. By administering ^{15}O-water and following the autoradiographic method (*14,15*), rCBF was estimated. Inhalation of ^{15}O-labeled carbon monoxide was performed to estimate rCBV. By inhaling ^{15}O-labeled molecular oxygen, rOEF and $rCMRO_2$ were obtained after blood volume correction (*16*). The details of the procedure are described elsewhere (*15*). The values of rCBF, $rCMRO_2$ and rOEF were estimated for the infarct, peri-infarct and remote areas (superior frontal gyrus), as well as the mirror regions in the contralateral hemisphere using 16-mm diameter circular ROIs.

Aphasia and Iomazenil Uptake

Patients 1, 5, 6 and 7 were aphasic. The aphasia was not transient. Patients 1 and 5 showed symptoms continuously throughout the chronic stage. Patients 1 and 7 showed global aphasia, Patient 5 motor aphasia and Patient 6 sensory aphasia. The Broca area of the inferior frontal gyrus for the global and motor aphasia (n = 3 patients) and the Wernicke area of the supramarginal gyrus for the global and sensory aphasias (n = 3 patients) were analyzed by examining the reference CT images and the L/C ratio for the SPECT images.

RESULTS

Iodine-123-Iomazenil Distribution

The reference CT image, blood flow image and iomazenil uptake of the cortical infarction (Fig. 1, Patient 6) and the subcortical white matter infarction (Fig. 2, Patient 7) are illustrated. In most cases of cortical infarction, a focal decrease in iomazenil uptake in the infarction and peri-infarct area was detected. The area of reduced iomazenil uptake was larger than the CT hypodense area in five of seven lesions of cortical infarction. Two patients were studied 8 (Patient 2) and 9 (Patient 3) days after onset. In these patients, the lesion was *partly* associated with elevated iomazenil uptake during the early phase after administration compared to the mirror region. Such lesions showed normal iomazenil uptake in the iomazenil image obtained 180 min after administration. Three lesions of subcortical infarction showed decreased iomazenil uptake in the adjacent cortex.

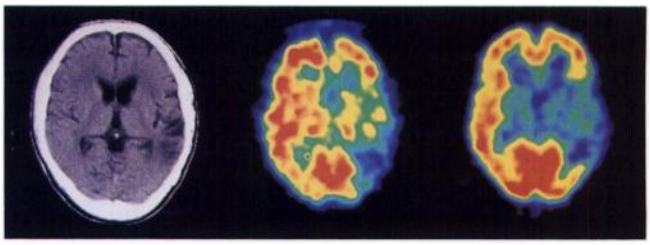

FIGURE 1. Patient 6. Reference CT (left), [^{123}I]IMP (center) and [^{123}I]iomazenil (right) images 40 mm above and parallel to the OM line. Cortical gray matter in the left temporal lobe was primarily affected as evidenced by CT hypodensity. Blood flow reduction was severe in the left MCA and was mild in the left anterior cerebral artery. Reduced iomazenil uptake extended beyond the CT hypodensity to the MCA. No right-left asymmetry of iomazenil uptake was found in the frontal lobe.

L/C Ratios for Iomazenil Uptake and Blood Flow

Figure 3 shows the L/C ratio of blood flow and iomazenil uptake for the infarct, peri-infarct and intrahemispheric remote areas and the cerebellum. Mean L/C ratio of the infarction was 0.52 ± 0.08 for blood flow and 0.53 ± 0.08 for iomazenil uptake. Both were significantly reduced compared with unity ($p < 0.001$). In the peri-infarct area, the ratio was 0.73 ± 0.07 for blood flow and 0.79 ± 0.07 for iomazenil uptake. Both values were significantly reduced when compared with unity ($p < 0.001$) and were increased when compared with those of the infarction ($p < 0.01$). No statistical difference was found between blood flow and

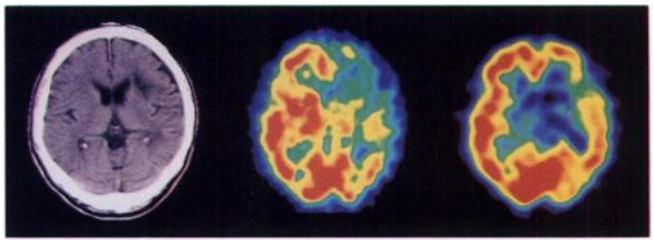

FIGURE 2. Reference CT image (left), [^{123}I]IMP image (center) and [^{123}I]iomazenil images (right) of the patient with subcortical infarction (no. 7). CT scan shows hypodensity in the frontal deep white matter with no involvement of the cortical area. Blood flow was reduced in the frontal and temporal cortices and in the basal ganglia and the thalamus. Iomazenil image demonstrates reduced uptake in the Broca area and more mild reduction in the frontal and temporal lobes that were normal on the CT images.

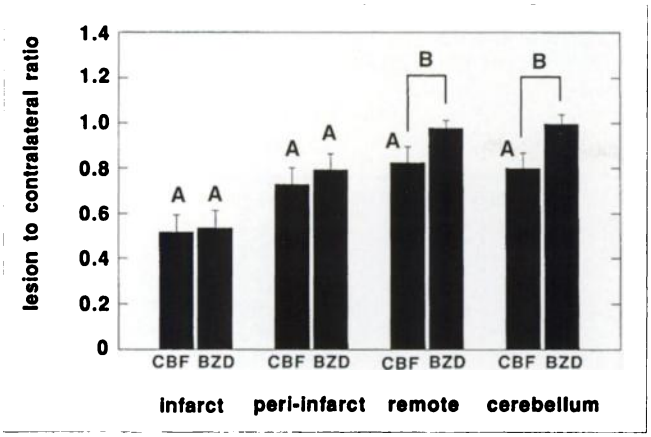

FIGURE 3. Mean L/C ratio of blood flow and iomazenil uptake in the infarct, peri-infarct and remote areas and the cerebellum. (A) Significant reduction compared with unity ($p < 0.001$). (B) Significant difference between CBF and iomazenil-BZD receptor binding ($p < 0.001$).

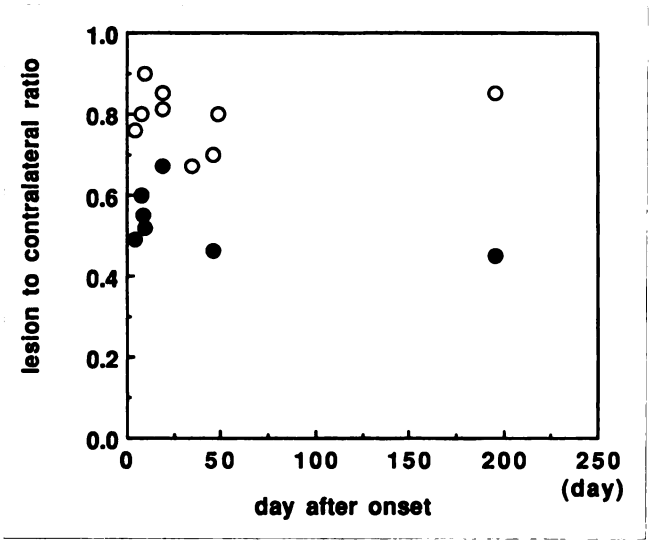

FIGURE 5. L/C ratio for the infarct (●) and peri-infarcted areas (○) plotted against the age after onset. L/C ratio was consistently below unity, irrespective of infarction age.

iomazenil uptake L/C ratios in either the infarct or peri-infarct areas. In the remote area, the ratio was 0.83 ± 0.09 for blood flow and 0.98 ± 0.03 for iomazenil uptake. Blood flow was significantly reduced compared with unity ($p < 0.001$) while iomazenil uptake was not. There was also a significant difference between the L/C ratio for blood flow and iomazenil uptake ($p < 0.001$). In the cerebellum, the contralateral-to-ipsilateral ratio was 0.80 ± 0.07 for blood flow and 1.00 ± 0.04 for iomazenil uptake. The L/C ratio for blood flow was significantly reduced compared with unity ($p < 0.001$). The blood flow ratio was also significantly lower than that for iomazenil uptake ($p < 0.001$). Figure 4 shows the cerebellar images of blood flow and iomazenil uptake obtained in Patient 7.

Age of Infarction and Iomazenil Uptake

In Figure 5, the L/C ratios for iomazenil uptake in the infarct and the peri-infarct areas are plotted against infarction age. There was no significant time-dependent change in the ratio for either area within the first 6 mo after onset.

CBF and $CMRO_2$ in the Infarct, Peri-infarct and Remote Areas

Figure 6 illustrates acute and chronic stage CT images,

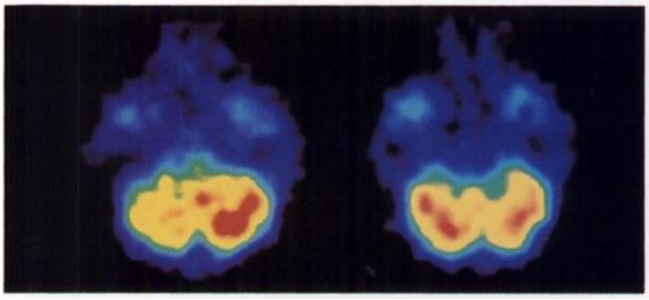

FIGURE 4. Iodine-123-IMP (left) and [^{123}I]iomazenil (right) images of the cerebellum in Patient 7, who had a left temporal lesion. In the right cerebellar hemisphere, blood flow was decreased by 20%, while iomazenil uptake was unchanged.

iomazenil uptake, rCBF, rOEF and $rCMRO_2$ for Patient 8. The right middle and inferior frontal gyri adjacent to the frontal deep white matter infarction showed CT normodensity where decreased iomazenil uptake, rCBF and $rCMRO_2$ were evident. The rOEF was not focally changed. Table 2 summarizes the mean values for the infarct, peri-infarct and remote areas as well as the mirror regions. Mean rOEF was not significantly different in the infarct, peri-infarct and remote areas.

Aphasia and Iomazenil Imaging

In the Broca area, the CT scan revealed faint hypodensity in one patient with motor aphasia (Patient 5) and normodensity in two patients with global aphasia (Patients 1 and 7). The mean L/C ratio of the Broca area in these

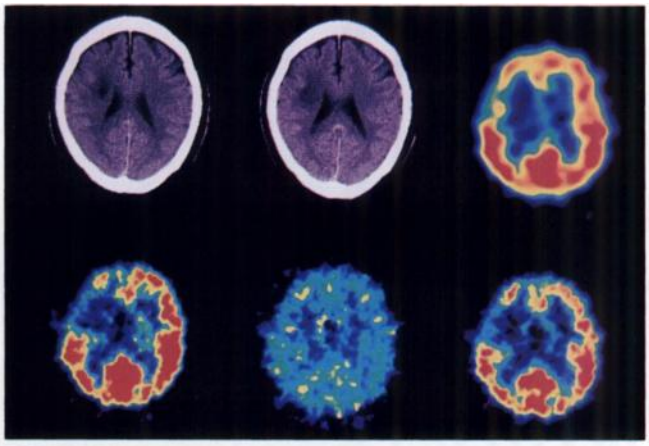

FIGURE 6. CT image at onset (top left) and during chronic stage (top center), iomazenil uptake (top right), rCBF (bottom left), rOEF (bottom center) and $rCMRO_2$ (bottom right) in Patient 8. Blood flow and oxygen consumption are decreased in the right frontal lobe, but iomazenil uptake is maintained in the territory of the anterior cerebral artery. No focal increase in extraction fraction was observed.

TABLE 2
Cerebral Blood Flow, Oxygen Extraction Fraction and Cerebral Oxygen Metabolic Rate for the Infarct, Peri-infarct and Remote Areas and the Mirror Region of the Contralateral Hemisphere

	Affected side			Contralateral mirror region		
	CBF	OEF	$CMRO_2$	CBF	OEF	$CMRO_2$
Infarction	25.8 ± 7.1*	0.39 ± 0.05	1.59 ± 0.29†	49.6 ± 1.9	0.46 ± 0.02	3.66 ± 0.46
Peri-infarct	34.7 ± 4.3*	0.43 ± 0.05	2.40 ± 0.46	50.0 ± 5.7	0.46 ± 0.05	3.44 ± 0.50
Remote area	39.2 ± 2.2	0.46 ± 0.06	2.88 ± 0.32	47.1 ± 5.6	0.45 ± 0.03	3.35 ± 0.17

*Significant difference ($p < 0.05$) compared with the mirror region.
†Significant difference ($p < 0.01$) compared with the mirror region.
CBF = cerebral blood flow; OEF = oxygen extraction fraction; $CMRO_2$ = cerebral oxygen metabolic rate.

patients was 0.68 ± 0.10 for blood flow and 0.63 ± 0.08 for iomazenil uptake. These values were significantly decreased compared with unity ($p < 0.001$). The Wernicke area showed CT hypodensity in Patients 1 and 6 and subcortical hypodensity in Patient 7. The mean L/C ratio was decreased to 0.51 ± 0.08 for blood flow and 0.56 ± 0.10 for iomazenil uptake, with statistical significance compared with unity ($p < 0.001$).

DISCUSSION

Central BZD Receptor Imaging

The central BZD receptor is a postsynaptic membrane receptor ionophore complex which contains a gamma-amino butyric acid (GABA) receptor (*17*). The GABA receptor mediates inhibitory signals in the regulation of cerebral function. The BZD/GABA receptor complex in the human brain was first measured in vivo with PET and ^{11}C-flumazenil (*18–20*). The observed distribution of BZD receptors in the brain was similar to that obtained in postmortem studies (*21*). Decreased BZD receptor density was associated with a reduction in neuron density in a histopathological study of traumatic brain injury (*22*). Carbon-11-flumazenil (*23*) and [^{123}I]iomazenil (*24*) radioactivity were displaced by pharmacological doses of these ligands. These studies indicate that central BZD receptor binding is a specific marker of the BZD/GABA mediating synapses of neurons. Imaging of the BZD receptor has been applied to several diseases. BZD receptor density was reduced in epileptogenic foci without any morphological abnormality in CT and MRI (*25*). Carbon-11-flumazenil binding was more sensitive and accurate for localization of epileptic foci than [^{18}F]FDG (*26*). A preliminary study indicated diminished iomazenil accumulation in patients with Alzheimer's disease (*27*).

Brain Ischemia and Central BZD Receptor Binding

Changes in BZD receptor binding resulting from transient brain ischemia were studied in the gerbil brain with ^{3}H-flunitrazepam autoradiography. In relation to histopathologic changes, diminished binding of ^{3}H-flunitrazepam was specifically observed in ischemic necrosis (*28*). BZD receptor binding was sensitive to ischemic damage, and preservation of BZD receptor binding soon after ischemia predicted the survival of brain tissue in the chronic phase. Middle cerebral artery occlusion in the rat yielded a more profound reduction in [^{125}I]iomazenil uptake than in blood flow measured by ^{99m}Tc-HMPAO 3 to 4 wk after the ictus (*29*). More recently, central BZD receptor change after focal ischemia was evaluated in vivo in baboon with serial PET studies and ^{11}C-flumazenil (*6*). A reduction in ^{11}C-flumazenil uptake in the infarcted area, produced by a unilateral middle cerebral artery occlusion, was found 2 days after onset and uptake continued to decrease up to 54 days. Similar findings were also observed for the peri-infarct area. A saturation study demonstrated that radioactivity in the infarction was less displaceable than that in intact brain, indicating that diminished ^{11}C-flumazenil uptake resulted from reduced receptor-ligand binding.

In the present study, iomazenil uptake was significantly decreased in the infarction identified as the CT hypodense area. In the peri-infarct CT normodense area, the reduction was less severe than in the infarction. Both the experimental (*6*) and human infarction indicated that ischemic damage extends beyond the CT hypodense lesion into the surrounding CT normodense area. The reduction in iomazenil uptake in the infarct and peri-infarct areas were associated with a decrease in CBF. In the ipsilateral superior frontal gyrus, however, a 17% reduction in the L/C ratio of CBF resulted in only a 2% decrease than that of iomazenil uptake. In the contralateral cerebellum, 20% reduction in the L/C ratio of CBF resulted in no decrease in that of iomazenil uptake. The discrepancy between iomazenil uptake and CBF in these areas, in addition to the preclinical study (*6*), indicated that the alteration in iomazenil uptake is not due to altered delivery but may predominantly reflect a receptor-mediated phenomenon.

Selective Neuronal Necrosis

Several neurohistological studies revealed that occlusion of the cerebral artery produces an infarction, total tissue necrosis, in the center of the ischemia, and neuron-specific alteration in the surrounding area. Mies et al. observed a decreased number of cortical neurons in the area surrounding experimentally produced chronic infarction in cat brain (*30*).

In a transient MCA occlusion model using the macaque

monkey, DeGirolami et al. (*31*) observed selective necrosis characterized by the disappearance of neuron cell bodies with preserved tissue framework, spared myelinated fibers and no evidence of vascular or intravascular abnormality in the area adjacent to or tapering away from the total tissue necrosis. Since neurons are more vulnerable to reduction of blood flow and oxygen deficiency than either glial cells or blood vessels (*32,33*), there may be a dividing ischemic threshold above which only neurons are specifically damaged. Although such neuron loss has not been confirmed in human autopsied brain (*34*), the reduction in iomazenil binding in the peri-infarct area may correspond to a selective neuronal necrosis. Lassen et al. observed neuronal loss in the CT normodense area in autopsied brain (*35*). They emphasized the importance of CT-negative irreversible ischemic damage, referred to as incomplete infarction, surrounding the ischemic center (*36*). Raynaud et al. also speculated that the mild reduction in CBF observed in the peri-infarct area of chronic infarction is due to selective neuronal necrosis, although deafferentiation cannot be ruled out completely (*37*). The present study supports this view and provides more direct evidence of neuronal damage in the peri-infarct area.

A reduction in iomazenil binding was found in the patient studied at 4 days after onset. In the baboon study, this reduction was not evident on Day 1, but was revealed on Day 2 (*6*). The time course of the acute stage reduction remains unknown for human infarction. Within a 6-mo period, however, all patients showed consistent reduction and no increase was found. This may indicate that damage observed by iomazenil binding is irreversible.

Aphasia and Iomazenil Imaging

CT has been used to depict the lesion responsible for clinical symptoms. In aphasia, there is good correlation between aphasia type and lesion localization (*38*). Various types of aphasia sometimes appear in patients without involving the classical language center of Broca and Wernicke on CT images (*39–41*). These studies assumed that lesions are confined to CT hypodensity. In such cases, the disconnection of specific neural pathways connecting the language center was considered. Metabolic measurement by PET (*42*) revealed that purely subcortical infarcts were accompanied by temporoparietal hypometabolism in patients with sensory aphasia, which supports the view that functional changes in undamaged cortical areas may underlie aphasia. Weiller et al. (*43*) studied 57 patients with strictly subcortical infarcts. Of these, patients with aphasia or neglect had a significantly longer duration of MCA occlusion and mostly poor leptomeningeal collaterals. The rCBF was significantly decreased in the cortical MCA territory in the patients with aphasia or neglect only. They speculated that aphasia or neglect after subcortical infarcts are most likely due to selective neuronal loss of the cerebral cortex due to prolonged MCA occlusion.

In the present study, one patient (no. 7) with global aphasia had purely subcortical lesions and significantly diminished iomazenil uptake in the CT-negative Broca and Wernicke areas (Fig. 2). Another globally aphasic patient (no. 1) had reduced iomazenil uptake in the CT-negative Broca area and in the CT hypodense Wernicke area. Our study indicated that not only the disconnection resulting from the CT lesion, but also CT-negative structural damage to the speech center, may be responsible for aphasia in these two patients.

Cerebral Perfusion, Metabolism and Iomazenil Uptake

Measurement of cerebral perfusion and metabolism in patients with infarction revealed a reduction in both parameters which spread far beyond the CT lesion (*44,45*). Although the number of patients was limited, we observed the same phenomenon. Regional CBF decreased by 48% in the infarction, 31% in the peri-infarcted area and 17% in the remote area. Although iomazenil uptake in the infarct and peri-infarct areas were reduced by the same magnitude as rCBF and $rCMRO_2$, normal iomazenil uptake was observed in the intrahemispheric remote area. These results are consistent with a previous study using ^{11}C-flumazenil in the baboon. Since no increase in oxygen extraction fraction was found, the hypoperfusion of the peri-infarct and remote areas was not a misery perfusion (*5*). In the peri-infarct area, hypoperfusion and hypometabolism may be due not to deafferentiation, but rather to an adaptation to neuron damage. In the ipsilateral superior frontal gyrus, reduced blood flow associated with normal iomazenil uptake might be an intrahemispheric remote effect of the infarction. The [^{123}I]iomazenil study may distinguish the extension of synaptic impairment from functionally inactivated and therefore hypoperfused lesions in the CT-normodense area outside the infarction.

Limitations

There are several methodological limitations in this study. Although quantitative evaluation of BZD receptor density and affinity was developed recently (*24,46*), we did not perform such analysis. Instead, we evaluated BZD receptor binding by taking the L/C ratio in the mirror region in the iomazenil image obtained 180 min postinjection. As indicated in the displacement trial in normal volunteers, more than 85% of cortical radioactivity 6 hr after injection was associated with specific binding to BZD receptors (*24*). Iomazenil images analyzed in this study may predominantly reflect specific binding. This does not, however, hold true under certain conditions after brain ischemia.

It is difficult to evaluate quantitatively the relative contribution of impaired delivery and reduced receptor density in the ischemic region by the L/C ratio analysis. For example, in luxury perfusion, nonspecific binding may correspondingly increase with increased delivery of the ligand, so that the fraction of nonspecific binding is higher than that in the reference region. Two patients studied at 8 and 9 days after onset had CT hypodensity associated, in part, with normal iomazenil uptake. These patients demonstrated a 20%–30% increase in the L/C ratio in iomazenil images obtained 15 min after injection, most likely as a

result of luxury perfusion. In such a case, the L/C ratio overestimates specific binding when images are taken before sufficient time has passed for nonspecific binding washout. Holthoff et al. separately estimated distribution volume, a measure corresponding to ligand-receptor binding potential, and the transport rate of ^{11}C-flumazenil by applying a two-compartment, two-parameter model (*47*). They demonstrated that the distribution volume is stable even if the delivery of ^{11}C-flumazenil is altered. Because of unstable and unexpected flow changes during the acute and subacute stages of cerebral infarction, such quantitative measurement should be carried out to avoid the uncertainty resulting from the flow dependency of the L/C ratio.

Another methodological limitation is that iomazenil is not sensitive to infarction in the central gray matter, subcortical white matter and brainstem as a result of the lower BZD receptor density in these areas (*17,24*).

CONCLUSION

Iodine-123-iomazenil uptake is decreased in cerebral infarction. This reduction extends to the surrounding CT normodense area. Reduced [^{123}I]iomazenil uptake in the peri-infarct area may be due to a selective neuronal necrosis not previously revealed by other imaging modalities. In the remote area and contralateral cerebellum, hypoperfusion was associated with normal [^{123}I]iomazenil uptake, indicating that neurons in these areas have normal synapses but are functionally deafferentiated. Therefore, [^{123}I]iomazenil SPECT provides new information on ischemic damage to the brain. Quantitative measurement of receptor density would further improve its accuracy.

ACKNOWLEDGMENTS

We thank Dr. Niels A. Lassen, Department of Clinical Physiology and Nuclear Medicine, Bispebjerg Hospital, Copenhagen, for his generous comments and valuable discussions about this study. We are grateful to the technical staff of the Department of Radiology and Nuclear Medicine. We also thank Y. Aizawa, T. Hachiya and Y. Shohji for preparing the photographs and Nihon Medi-Physics, Hyogo, Japan, for providing the [^{123}I]iomazenil.

REFERENCES

1. Drayer BP, Rosenbaum AE. Brain edema defined by cranial computed tomography. *J Comput Assist Tomogr* 1979;3:317–323.
2. Sipponen JT, Kaste M, Ketonen L, Sepponen RE, Katevuo K, Sivula A. Serial nuclear magnetic resonance (NMR) imaging in patients with cerebral infarction. *J Comput Assist Tomogr* 1983;7:585–589.
3. Shimosegawa E, Hatazawa J, Inugami A, et al. Cerebral infarction within six hours of onset: prediction of completed infarction with technetium-99m-HMPAO SPECT. *J Nucl Med* 1994;35:1097–1103.
4. Hanson SK, Grotta JC, Rhoades H, et al. Value of single-photon emission-computed tomography in acute stroke therapeutic trials. *Stroke* 1993;24: 1322–1329.
5. Baron JC. Positron tomography in cerebral ischemia: a review. *Neuroradiology* 1985;27:509–516.
6. Sette G, Baron JC, Young AR, et al. In vivo mapping of brain benzodiazepine receptor changes by positron emission tomography after focal ischemia in the anesthetized baboon. *Stroke* 1993;24:2046–2058.
7. Beer HF, Blauenstein PA, Hasler PH, et al. In vitro and in vivo evaluation of Iodine-123-Ro 16-0154: a new imaging agent for SPECT investigations of benzodiazepine receptors. *J Nucl Med* 1990;31:1007–1014.
8. Woods SW, Seibyl JP, Goddard AW, et al. Dynamic SPECT imaging after injection of the benzodiazepine receptor ligand [^{123}I]iomazenil in healthy human subjects. *Psych Res* 1992;45:67–77.
9. Johnson EW, Woods SW, Zoghbi S, McBride BJ, Baldwin RM, Innis RB. Receptor binding characterization of the benzodiazepine radioligand [^{123}I]Ro 16-0154: potential probe for SPECT brain imaging. *Life Sci* 1990; 47:1535–1546.
10. Innis R, Zoghbi S, Johnson E, et al. SPECT imaging of the benzodiazepine receptor in nonhuman primate brain with [^{123}I]Ro 16-0154. *Eur J Pharmacol* 1993;193:249–252.
11. Dey HM, Seibyl JP, Stubbs JB, et al. Human Biodistribution and dosimetry of the SPECT benzodiazepine receptor radioligand iodine-123-iomazenil. *J Nucl Med* 1994;35:399–404.
12. Iida H, Itoh H, Nakazawa M, et al. Quantitative mapping of regional cerebral blood flow using [^{123}I]N-isopropyl-p-iodoamphetamine and single-photon emission tomography. *J Nucl Med* 1994;35:2019–2030.
13. Lassen NA, Andersen AR, Neirinckx RD, Ell PJ, Costa DC. Validation of Ceretec. In: Ell JP, Costa DC, Cullum ID, Jarritt PH, Lui D, eds. *rCBF atlas—the clinical application of rCBF imaging by SPECT*. High Wycombe: Brier Press; 1987:14–18.
14. Raichle ME, Martin WRW, Herscovitch P, Mintun MA, Markham J. Brain blood flow measured with intravenous H2^{15}O. II. Implementation and validation. *J Nucl Med* 1983;24:790–798.
15. Kanno I, Iida H, Miura S, et al. A system for cerebral blood flow measurement using H2^{15}O autoradiographic method and positron emission tomography. *J Cereb Blood Flow Metab* 1987;7:143–153.
16. Mintun MA, Raichle ME, Martin WRW, Herscovitch P. Brain oxygen utilization measured with O-15 radiotracers and positron emission tomography. *J Nucl Med* 1984;25:177–187.
17. Olsen RW. The GABA postsynaptic membrane receptor-ionophore complex. *Mol Cell Biochem* 1981;39:261–279.
18. Samson Y, Hantraye P, Baron JC, Soussaline F, Comar D, Maziere M. Kinetics and displacement of ^{11}C-Ro 15-1788, a benzodiazepine antagonist, studied in human brain in vivo by positron emission tomography. *Eur J Pharmacol* 1985;110:247–251.
19. Persson A, Ehrin E, Eriksson L, et al. Imaging of [^{11}C]-labeled RO 15-1788 binding to benzodiazepine receptors in the human brain by positron emission tomography. *J Psychiat Res* 1985;19:609–622.
20. Shinotoh H, Yamasaki T, Inoue O, et al. Visualization of specific binding sites of benzodiazepine in human brain. *J Nucl Med* 1986;27:1593–1599.
21. Richards JG, Mohler H. Benzodiazepine receptors. *Neuropharmacology* 1984;23:233–242.
22. Benavides J, Serrano A, Duval D, Bourdiol F, Toulmond S, Scatton B. Autoradiographic detection and quantitation of traumatic brain lesions in the rat brain by using site radioligands. In: Kriegstein J, Oberpichler H, eds. *Pharmacology of cerebral ischemia*. Stuttgart: Wissenschaftliche Verlagsgesellschaft mbH; 1989:39–45.
23. Persson A, Ehrin E, Eriksson L, et al. Imaging of [^{11}C]-labeled RO-15-1788 binding to benzodiazepine receptors in the human brain by positron emission tomography. *J Psychiat Res* 1985;19:609–622.
24. Abi-Dargham A, Lauruelle M, Seibyl J, et al. SPECT measurement of benzodiazepine receptors in human brain with iodine-123-iomazenil: kinetic and equilibrium paradigms. *J Nucl Med* 1994;35:228–238.
25. Savic I, Roland P, Sedvall G, Persson A, Paulis S, Widen L. In vivo demonstration of reduced benzodiazepine receptor binding in human epileptic foci. *Lancet* 1988;2:863–866.
26. Savic I, Ingvar M, Stone-Elander S. Comparison of [^{11}C]flumazenil and [^{18}F]FDG as PET markers of epileptic foci. *J Neurol Neurosurg Psych* 1993; 56:615–621.
27. Schubiger PA, Hasler PH, Beer-Wohlfahrt H, et al. Evaluation of a multicentre study with iomazenil: a benzodiazepine receptor ligand. *Nucl Med Commun* 1991;12:569–582.
28. Onodera H, Kogure K. GABA and benzodiazepine receptors in the gerbil brain after transient ischemia: demonstration by quantitative receptor autoradiography. *J Cereb Blood Flow Metab* 1987;7:82–88.
29. Matsuda H, Tsuji S, Kuji I, Hisada K. Central type benzodiazepine receptor and cerebral blood flow in experimental chronic brain infarction—evaluation using a double-tracer autoradiography technique. *Jpn J Nucl Med* 1993; 30:643–650.
30. Mies G, Auer LM, Ebhardt G, Traupe H, Heiss WD. Flow and neuronal density in tissue surrounding chronic infarction. *Stroke* 1983;14:22–27.
31. DeGirolami U, Crowell RM, Marcoux FW. Selective and total necrosis in focal cerebral ischemia. Neuropathologic observations on experimental middle cerebral artery occlusion in the macaque monkey. *J Neuropath Exp Neurol* 1984;43:57–71.
32. Jacob H. CNS tissue and cellular pathology in hypoxaemic states. In: Schade

JP, McMenemey WH, eds. *Selective vulnerability of the brain in hypoxemia.* Oxford: Blackwell Scientific; 1963:153–163.
33. Graham DI. Hypoxia and vascular disorders. In: Adams JH, Duchen LW, eds. *Greenfield's neuropathology*, 5th ed. London: Edward Arnold; 1992:153–268.
34. Nedergaard MN, Vorstrup S, Astrup J. Cell density in the border zone around old small human brain infarcts. *Stroke* 1986;17:1129–1136.
35. Lassen NA, Olsen TS, Hojgaard K, Skriver E. Incomplete infarction: a CT-negative irreversible ischemic brain lesion. *J Cereb Blood Flow Metab* 1983;3:S602–603.
36. Lassen NA. Incomplete cerebral infarction—focal incomplete ischemic tissue necrosis not leading to emollision. *Stroke* 1982;13:522–523.
37. Raynaud C, Rancurel G, Samson Y, et al. Pathophysiologic study of chronic infarcts with I-123-isopropyl iodo-amphetamine (IMP): the importance of periinfarct area. *Stroke* 1987;18:21–29.
38. Naeser MA, Hayward RW. Lesion localization in aphasia with cranial computed tomography and the Boston Diagnostic Aphasia Exam. *Neurology* 1978;28:545–551.
39. Vignolo LA, Boccardi E, Caverni L. Unexpected CT scan findings in global aphasia. *Cortex* 1986;22:55–69.
40. Naeser M, Alexander MP, Helm-Estabrooks N, Levine H, Laughlin SA, Geschwind N. Aphasia with predominantly subcortical lesion sites: description of three capsular/putaminal aphasia syndromes. *Arch Neurol* 1982;39:2–14.
41. Alexander MP, Naeser M, Palumbo CL. Correlations of subcortical CT lesion sites and aphasia profiles. *Brain* 1987;110:961–991.
42. Karbe H, Herholz K, Szelies B, Pawlik G, Wienhard K, Heiss WD. Regional metabolic correlates of Token test results in cortical and subcortical left hemispheric infarction. *Neurology* 1989;39:1083–1088.
43. Weiller C, Willmes K, Reiche W, et al. The case of aphasia or neglect after striatocapsular infarction. *Brain* 1993;116:1509–1525.
44. Kuhl DE, Phelps ME, Kowell AP, Metter EJ, Selin C, Winter J. Effects of stroke on local cerebral metabolism and perfusion: mapping by emission computed tomography of ^{18}FDG and $^{13}NH_3$. *Ann Neurol* 1980;8:47–60.
45. Lenzi GL, Frackowiak RSJ, Jones T. Cerebral oxygen metabolism and blood flow in human cerebral ischemic infarction. *J Cereb Blood Flow Metab* 1982;2:321–335.
46. Laruelle M, Adi-Dargham A, Al-Tikriti MS, et al. SPECT quantification of [^{123}I]iomazenil binding to benzodiadepine receptors in nonhuman primates: II. Equilibrium analysis of constant infusion experiments and correlation with in vitro parameters. *J Cereb Blood Flow Metab* 1994;14:453–465.
47. Holthoff VA, Koeppe RA, Frey KA, et al. Differentiation of radioligand delivery and binding in the brain: validation of a two-compartment model for [^{11}C]flumazenil. *J Cereb Blood Flow Metab* 1991;11:745–752.

Scatter

(Continued from page 3A)

"Well of course we want to be consistent with JAMA."

"As I suspected. Not very original, are you? You should be more original in your standards. Try something innovative!"

"What do you mean?"

"I noticed that all of your articles contain many references. Why don't you eliminate them?"

"You're supposed to reference the ideas of others. That avoids accusations of plagiarism."

"Well, you can't have it both ways. You want your articles to be original, but you won't let the authors claim their ideas are 'new' or 'the first observation', and then you make them reference everything. How can you do that and claim that everything you publish is original? Anyway, your reviewers criticize everything new. They usually don't believe something that hasn't been observed before."

"I'm not finding you very helpful. I had hoped that I could rely on the integrity and competence of the authors, reviewers and editorial board members, including me. What's wrong with that?"

"How long have you been lost in these woods?"

Stanley J. Goldsmith, MD
Editor-in-Chief, The Journal of Nuclear Medicine
December 1995